Automatic Learning Control for Unbalance Compensation in Active Magnetic Bearings

Chao Bi, *Member, IEEE*, Dezheng Wu, *Student Member, IEEE*, Quan Jiang, *Member, IEEE*, and Zhejie Liu, *Senior Member, IEEE*

MRC Division, A*Star Data Storage Institute, Singapore 117608, Singapore

This paper proposes a new control scheme, automatic learning control, to eliminate unbalance effects, which adversely affect the operation of active magnetic bearings. This control method is based on time-domain iterative learning control and gain-scheduled control. The controller can utilize the optimal control currents for the unbalance compensations. In addition, the variable learning cycle and variable learning gain are employed in the learning process to achieve better performance against rotating speed fluctuations. The control algorithm does not require large memory size and intensive computation. We tested the control system in experiments, and the experimental results prove that the control method is effective over a wide range of operation speeds.

Index Terms—**Active magnetic bearings, automatic learning control, unbalance compensation.**

I. Introduction

UNBALANCE effects are normally a concern in rotating machinery. When a rotor's geometric axis, inertial axis and an actuator's magnetic axis are not coincident, the synchronous unbalance force will be induced and it can result in rotor position runout and machine housing vibrations, especially for the vibrations with critical frequencies [1]. The conventional method of balancing is realized by employing mechanical approaches, for example, the addition or removal of a small amount of mass from the rotor to reduce the residual imbalance. The mechanical balancing is a time-consuming and costly procedure. In addition, the imbalance often changes during operation in some machines and the mechanical balancing has limited benefits in this case [2]. An active magnetic bearing (AMB), which levitates a rotating object (typically, a rotor in electric machines) in a magnetic field, is proven to be a good solution to this kind of unbalance problem. With effective control methods, AMB can generate electromagnetic (EM) forces to actively control the movement of rotor; thus, the unbalance effects can be greatly attenuated in machines with AMB.

Since unbalance disturbance is common in rotating machinery and it degrades system performance, AMB researchers pay much attention to this problem, seeking control strategies to attenuate unbalance effects in AMB. Various unbalance compensation techniques have been developed since the last decade [2]–[11]. Early unbalance control techniques were based on insertion of notched filters in the control loop. The major drawback of this method is that the notch filters affect the stability of the control system so that they can be used in only a limited speed range. A generalized notch filter was then proposed to overcome this problem [3]. The generalized notch filter has the advantage in free pole location, which can enable the filter to process the synchronous unbalance signals at different rotational speeds. Some designs, which are based on the state feedback control approach, are also developed to stabilize the system with the ability of unbalance disturbance rejection [4], [5]. State observers were used in these designs to estimate the state variables which cannot be directly measured by sensors. However, as pointed out by [6], both notch filter approach and observer-based state feedback approach have the drawback that they alter the complementary sensitivity function of the system such that the stability of the AMB system is worsened. Later, more research works were focused on designing an "add-on" controller that may be added to conventional feedback controllers without altering the system stability or performance. To attenuate the unbalance effects, this kind of additional controller should be able to produce a synchronous control signal according to unbalance signals. Some control schemes based on adaptive control are developed to generate this synchronous compensation input [6]–[8]. Frequency-domain iterative learning control (FILC) has also been applied in active magnetic bearings [9]. Knopse *et al.* proposed an adaptive vibration control (AVC) method which is similar to the frequency-domain iterative learning control [2]. AVC incorporates a look-up table of gain matrices into the iterative learning law and selects a gain matrix according to operation conditions. This look-up table simplifies the control algorithm by waiving the process of online estimation in each cycle, but it requires much memory space which is difficult in many applications, especially for the system operating over a wide-speed range, like the spindle motors used in hard disk drives. Therefore, several strategies were then proposed for relieving its memory requirements [10].

Various methods have been developed and most of the schemes can provide satisfying control effects. However, most of the existing methods require the precise prior knowledge of AMB parameters, which may be unique for each AMB due to manufacturing errors. Moreover, most of the existing unbalance control approaches are so complicated that they require the intensive computational effort or large memory space in digital processors, which limit the application of these approaches. For example, the DSP in hard disk drives already needs to process many issues such as coding, spindle motor drive, servo control, etc. It is not practical to additionally impose much computation load or large memory space requirements for AMB control

Digital Object Identifier 10.1109/TMAG.2005.851866

when the AMB spindle motor is used. As a result, a practical unbalance control technique, which does not rely much on the capability of digital processors while providing excellent control effect, is needed for AMB unbalance compensation. In this paper, a control scheme, automatic learning control (ALC), is presented to compensate the unbalance in AMB. ALC is based on time-domain iterative learning control (ILC). Variable learning cycles (or trials) and gains for different speeds are used instead of fixed ones in the learning law to enable controller to work in a wide range of speeds. Another advantage of this control scheme is that it has better transient performance against rotational speed disturbances. Experimental results prove the effectiveness of ALC scheme in a wide range of rotational speeds.

II. AMB Model and Unbalance Analysis

A totally suspended magnetic bearing system is composed of five degree-of-freedom (DOF) suspensions, i.e., four radial DOF controlled by two identical radial bearings and an axial DOF controlled by a thrust bearing. An AMB system is usually arranged in such a way that the axial subsystem can be totally separated from other radial subsystems. Furthermore, because the unbalance effects appear in radial directions, only motions in the four radial DOF will be analyzed in this paper. To simplify the description, in this section, only one radial bearing is analyzed to show the unbalance problem in the AMB system. The other radial bearings have similar unbalance effects. Fig. 1 shows a two-DOF closed-loop radial AMB system. Position sensors are used to detect the rotor position in both DOFs. A controller receives position signals and generates corresponding control currents to stabilize the AMB system, which means currents in the two opposite electromagnet coils are $i_1 = i_0 + i_c, i_2 = i_0 - i_c$ respectively, where i_0 is the bias current and i_c is the control current. The EM force in an axis can be therefore expressed as [12]

$$f_m = K_m \cdot \left[\frac{i_1^2}{(s_0 - s)^2} - \frac{i_2^2}{(s_0 + s)^2} \right] \tag{1}$$

where K_m is a constant related to AMB structure and core materials of the electromagnet, s_0 is the air gap when the rotor is in the central position, and s is the rotor displacement with respect to the bearing center in this axis. Thus, $(s_0 - s)$ and $(s_0 + s)$ are respectively the air gaps for the two opposite electromagnets.

This EM force can be linearized at the equilibrium point where $i_c = i_{c0}, s = 0$, and the equation becomes

$$f_m = K_i \cdot i_c + K_s \cdot s \tag{2}$$

where

$$\begin{cases} K_i \triangleq \dfrac{\partial}{\partial i_c} f_m \Big|_{i_c = i_{c0}, s = 0} = \dfrac{4K_m i_0}{s_0^2} \\ K_s \triangleq \dfrac{\partial}{\partial s} f_m \Big|_{i_c = i_{c0}, s = 0} = \dfrac{4K_m \left(i_0^2 + i_{c0}^2\right)}{s_0^3} \end{cases}. \tag{3}$$

If there is external constant force acting at the rotor, e.g., the gravity force, a constant partial of the control current, i_{c0}, will be generated by the proportional-integral-derivative (PID) control circuit to compensate the external force.

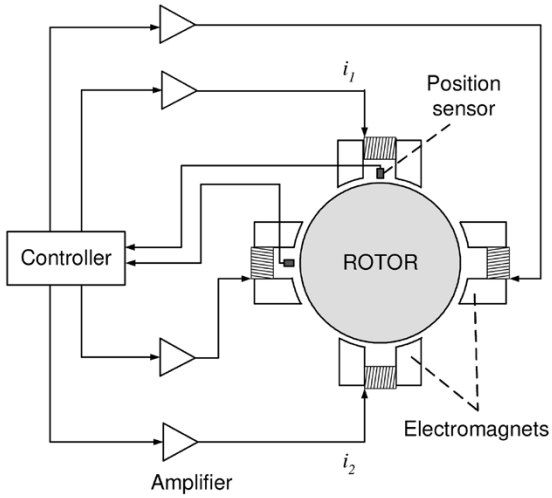

Fig. 1. Structure of a two-DOF AMB system.

If the AMB is permanent-magnet-biased, where the bias flux generated by permanent magnets (PMs) replaces bias current to produce the same effect, the EM force formula has the same format as (2). The difference is that for a PM-biased magnetic bearing, the force-current factor K_i and force-displacement factor K_s in (2) are related to permanent-magnet parameters instead of the bias current [13]. The results in this paper can be easily extended to the case where the PM-biased magnetic bearing is used.

If there are no other forces except the magnetic bearing force, according to Newton's law, the motion of the rotor can be described by

$$m\ddot{s} = f_m - f_w = (K_i \cdot i_c + K_s \cdot s) - f_w \tag{4}$$

where f_w is the partial weight of the rotor in one DOF, and m is the mass of the rotor.

Therefore, the motion equation for AMB plant can be expressed in the state–space form as

$$\begin{bmatrix} \dot{s} \\ \ddot{s} \end{bmatrix} = \begin{bmatrix} 0 & 1 \\ \frac{K_s}{m} & 0 \end{bmatrix} \begin{bmatrix} s \\ \dot{s} \end{bmatrix} + \begin{bmatrix} 0 \\ \frac{K_i}{m} \end{bmatrix} \left(i_c - \frac{f_w}{K_i} \right). \tag{5}$$

Because EM forces in AMB are inherently open-loop unstable, a negative feedback controller, usually a PID controller, must be used to realize the stable control of rotor position. However, periodical disturbance forces acting on the rotor, for example, the unbalance force resulting from the unalignment between the geometric center and mass center of the rotor, could induce the periodical runout of the rotor if only the PID control is applied. The runout of the rotor is generated as the following analysis.

In order to explain how the unalignment between the mass center and geometric center of the rotor causes the periodical runout of the rotor surface, the 2-D plan AMB in Fig. 2 is taken as an example, with the geometric center $O_{\rm gm}$, mass center $O_{\rm in}$, the mass eccentricity ε, and rotor angular speed ω. The unbalance force due to this mass eccentricity can be modeled as

$$f_{mx} = [s_x + \varepsilon \cos(\omega t + \theta)] m\omega^2 \tag{6}$$

$$f_{my} = [s_y + \varepsilon \sin(\omega t + \theta)] m\omega^2 \tag{7}$$

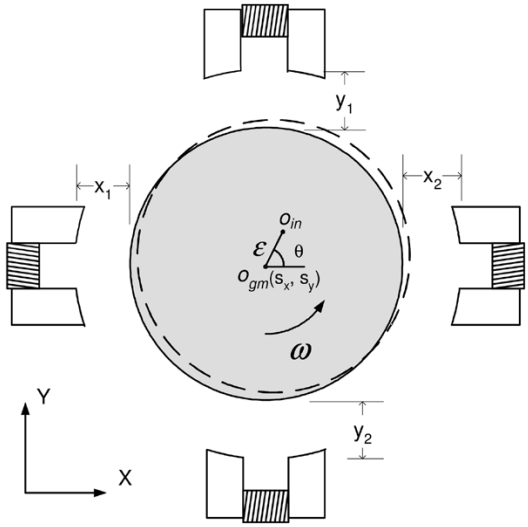

Fig. 2. Mass unbalance in AMB.

where the point (s_x, s_y) is the position of rotor geometric center and θ is the initial phase of unbalance forces. When $s_x \neq 0$ and/or $s_y \neq 0$, there also exists EM unbalance in AMB. At this moment, the geometric axis does not coincide with the EM axis and their centers have a displacement of (s_x, s_y).

Similar to (4), applying Newton's law, the motion equations of rotor in both X and Y axes are

$$m\ddot{s}_x = [s_x + \varepsilon\cos(\omega t + \theta)]m\omega^2 + K_s \cdot s_x + K_i \cdot i_{cx} - f_{wx} \tag{8}$$

$$m\ddot{s}_y = [s_y + \varepsilon\sin(\omega t + \theta)]m\omega^2 + K_s \cdot s_y + K_i \cdot i_{cy} - f_{wy} \tag{9}$$

where f_{wx} and f_{wy} are the partial weights of rotor in axis X and axis Y, respectively. Equations (8) and (9) are based on the assumption that the cross section of the rotor is perfectly round. Otherwise higher-order harmonic components would appear in the right side of the equations, and they could excite higher order EM unbalance forces in AMB.

Consider the case where the AMB system is designed to keep f_{wx} and f_{wy} equal, the weight balancing current i_{c0} could be

$$i_{c0} = \frac{f_{wx}}{K_i} = \frac{f_{wy}}{K_i}. \tag{10}$$

Then the motion equations (8) and (9) can be rewritten as

$$m\ddot{s}_x = [s_x + \varepsilon\cos(\omega t + \theta)]m\omega^2 + K_s \cdot s_x + K_i \cdot (i_{cx} - i_{c0}) \tag{11}$$

$$m\ddot{s}_y = [s_y + \varepsilon\sin(\omega t + \theta)]m\omega^2 + K_s \cdot s_y + K_i \cdot (i_{cy} - i_{c0}). \tag{12}$$

In X and Y DOFs, assuming that their PID control parameters are same, we can get

$$i_{cx} = -k_P s_x - k_D \dot{s}_x - k_I \int_0^t s_x \, d\tau \tag{13}$$

$$i_{cy} = -k_P s_y - k_D \dot{s}_y - k_I \int_0^t s_y \, d\tau \tag{14}$$

where k_P, k_I, and k_D are the PID control parameters.

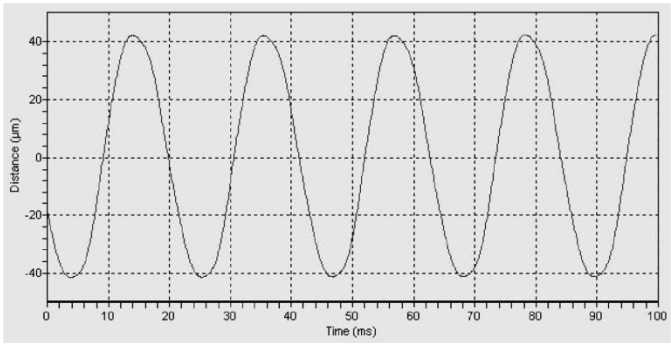

Fig. 3. Runout curve of one DOF.

Solving (11)–(14), the fundamental component of the runout could be derived as follows:

$$\begin{cases} s_x(t) = C_\omega \cos(\omega t + \delta_\omega), \\ s_y(t) = C_\omega \sin(\omega t + \delta_\omega) \end{cases} \tag{15}$$

where

$$C_\omega = \frac{m\varepsilon\omega^3 \cos\theta}{\omega[K_i(k_P + k_D) - K_s - 2m\omega^2]\cos\delta_\omega + K_i k_I \sin\delta_\omega} \tag{16}$$

$$\delta_\omega = \theta + \tan^{-1}\left[\frac{K_i k_I}{K_i(k_P + k_D)\omega - K_s\omega - 2m\omega^3}\right]. \tag{17}$$

They show that, if the initial angle θ is not $\pi/2$ or $3\pi/2$, the oscillation of the rotor center and the periodical runout must appear if only PID control is applied. The experimental result in Fig. 3 also confirms this phenomenon.

In real cases, the cross section of rotor may not be perfectly round. This will make the runout curves in X and Y directions different in their amplitudes.

The mass unbalance in AMB is due to the faults in manufacturing procedures, or the quality of the components used. Reducing the manufacturing faults is always concerned, but the mechanical and material processes are not enough in many high-performance applications. In these cases, the active rotor balancing technique can supply a satisfied solution.

Typically, unbalance compensation in AMB is carried out in two ways: reduction of rotor runout and reduction of coil current fluctuations. The former one is quite significant for the applications that require a high level of rotational accuracy. When the unbalance force is well counteracted by AMB, the rotor is strictly rotating around on its geometric axis and its runout is reduced to zero. Reducing coil current fluctuation in AMB has the advantage of attenuating the transmission of synchronous forces to the bearing housing [9]. When the rotor rotates, the unbalance forces caused by the acceleration of the inertial axis and the unsymmetrical magnetic field are reacted by the magnetic bearing and transmitted to the housing. One approach to solve this problem is to make the rotor rotate around on its system inertial axis. System inertial axis is defined in this paper to represent a virtual axis such that if the rotation is about system inertial axis, no force due to unbalance is transmitted to the housing. Elimination of current fluctuations in AMB coils means that the unbalance has no influence on AMB actuator. So the rotor is well balanced and rotates about its system inertial axis. Another advantage of reducing current fluctuation is the significant saving

of copper loss in PM-biased magnetic bearings [14]. In this paper, both compensation modes will be realized with learning control schemes.

III. Time-Domain Iterative Learning Control Scheme

Iterative learning control was first developed with the objective of eliminating periodic tracking errors in robots [15]. Because of its attractive characteristics, ILC has become increasingly popular since its birth in 1984. Recently, ILC has been applied in various applications, such as robotic manipulators and motor control [16], [17].

The basic idea of ILC is to improve the control performance of the present cycle by incorporating past control information in current control input, and this is very different from most other control methods. In ILC, the controller first calculates e_j, the difference between the system output y_j and the desired output y_d. Then the controller yields a new input u_{j+1} for the next cycle according to the learning law. The new input is temporarily stored in the memory. In this process, the new input is the sum of the old input in previous cycle and an error correction item, and the input can make the tracking error e_j be decreased cycle by cycle. Through this learning process, a desired input signal could be finally obtained and the error can therefore be minimized.

A general iterative learning law in time domain can be described by

$$u_{j+1}(n) = u_j(n) + \Phi \cdot e_j(n), \quad n \in 0, 1, 2, \ldots, n_f - 1 \tag{18}$$

where n_f is the number of sampling points in one cycle, $u(n)$ is the controller input, j is iteration (or cycle) number, the scalar Φ is defined as the learning gain, and the error is

$$e_j(n) = y_d(n) - y_j(n). \tag{19}$$

Typically, a discrete-time closed-loop AMB system model of one DOF has a state–space form of

$$\begin{cases} \mathbf{X}(n) = \mathbf{A} \cdot \mathbf{X}(n-1) + \mathbf{B} \cdot \mathbf{u}(n-1) \\ \mathbf{Y}(n) = \mathbf{C} \cdot \mathbf{X}(n) \end{cases}. \tag{20}$$

The details of $\mathbf{A}, \mathbf{B}$, and $\mathbf{C}$ are explained in the Appendix.

According to the convergence condition [18], if the learning gain in (18) satisfies

$$|1 - b_{11}\Phi| < 1 \tag{21}$$

thus for all $n \in [0, n_f - 1]$

$$\lim_{j \to \infty} e_j(n) = \lim_{j \to \infty} [y_d(n) - y_j(n)] = 0. \tag{22}$$

Actually, the system model parameters could be ignored in the process of determining the learning gain. A suitable learning gain able to yield the required performance can be easily obtained by online tuning like tuning a PID controller. The detailed method of choosing a learning gain is discussed in [19].

To improve the robustness of the controller, a forgetting factor α is introduced in the learning process to increase the robustness of the learning control algorithm against the noise, jumps of the unbalance forces, rotor speed variation, and other unknown perturbations. The reasons for using such a factor have been elaborated in detail by [20]. A negative effect of forgetting factor is that it can weaken the compensation effect of iterative learning control, making final error not converge to zero. The larger the forgetting factor is, the larger the final error is but the more robust the learning controller is. Therefore, α should be selected at a balance value to produce acceptable compensation effect as well as satisfactorily adequate robustness of the iterative learning controller. The learning controller with a forgetting factor becomes

$$u_{j+1}(n) = (1 - \alpha)u_j(n) + \Phi \cdot e_j(n). \tag{23}$$

To reduce the rotor runout, the displacement signal $e_{p,j}$ is the controller input for ILC. From (23), the learning controller for reducing rotor runout is

$$\begin{aligned} i_{\mathrm{ILC},j+1}(n) &= (1 - \alpha) i_{\mathrm{ILC},j}(n) + \Phi \cdot e_{p,j}(n) \\ &= (1 - \alpha) i_{\mathrm{ILC},j}(n) - \Phi \cdot s_j(n) \end{aligned} \tag{24}$$

where i_{ILC} is the AMB current generated by ILC controller and s_j is the rotor position with the unbalance disturbance.

To reduce the current fluctuation, the current fluctuation signal e_i is the controller input for ILC. The learning controller for reducing current fluctuation can be described as

$$\begin{aligned} i_{\mathrm{ILC},j+1}(n) &= (1 - \alpha) i_{\mathrm{ILC},j}(n) + \Phi \cdot e_{i,j}(n) \\ &= (1 - \alpha) i_{\mathrm{ILC},j}(n) - \Phi \cdot i_{\mathrm{syn},j}(n) \end{aligned} \tag{25}$$

where $i_{\mathrm{syn},j}$ is the corresponding synchronous control current for the rotor's displacement, which is ac component of PID control currents in (13) and (14) when the rotor has the runout.

IV. Automatic Learning Control Scheme

The ILC unbalance compensation scheme introduced in Section III is developed for a fixed rotational speed. This controller is not suitable for the case where the motor speed has fluctuation. In addition, the ILC scheme in Section III is not robust to the speed disturbance. All these limit the application of the proposed ILC controller. The errors of the speed sensor are also the source to cause speed signal fluctuation. To improve the robustness of the ILC scheme and make AMB capable of working over a wide-speed range, the following control scheme which is defined as automatic learning control (ALC) is proposed. The main ideas of ALC are composed of the following improvements.

1) Learning gains for different rotational speeds are stored in a look-up table and are used iteratively during AMB operation.
2) Obtain the fundamental component from the original position signal or current signal.
3) Use an interpolation method to compute the corresponding learning gains for the current rotational speed.
4) Change the length of learning cycle with rotation speed and keep it always equal to the rotation period.

The learning gains and the length of a learning cycle are automatically determined in Step 3) and Step 4), respectively. Therefore, ALC can automatically adjust the gain and the cycle length itself during operation to make it suitable for working at the current rotational speed.

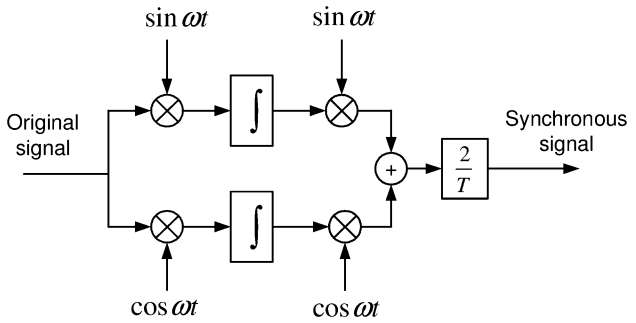

Fig. 4. Synchronous signals processing unit.

A. Process Synchronous Signals

Generally in ILC, a low-pass filter is required because the high-frequency noise could make the learning process unstable. In ALC, the controller works in a wide range of motor speeds, so the filter should be able to obtain synchronous components from original runout and current ripple signals at different speeds. Fourier analysis technique is used in ALC to process the synchronous signal. The synchronous signal can be obtained according to the following:

$$a = \frac{2}{T}\int_{t_0}^{T+t_0} y_o(t)\sin(\omega t)\,\mathrm{d}t \tag{26}$$

$$b = \frac{2}{T}\int_{t_0}^{T+t_0} y_o(t)\cos(\omega t)\,\mathrm{d}t \tag{27}$$

$$y_\omega(t) = a\cdot\sin\omega t + b\cdot\cos\omega t \tag{28}$$

where $y_o(t)$ is the original signal, $y_\omega(t)$ is the synchronous signal, ω is the rotational angular velocity, T is the rotational period, a is the amplitude of synchronous sine wave, and b is the amplitude of synchronous cosine wave. The process of obtaining synchronous components is shown in Fig. 4.

B. Gain-Scheduled Control

The variation of rotational speed could lead to the variation of AMB plant parameters [12], so a learning gain may be effective at one rotating speed but may lead to instability at another speed. To solve this problem, in the required speed range, the controller in ALC should be able to adjust its learning gain to different rotational speeds. Gain-scheduled control is employed to achieve different learning gains according to the rotating speed. The learning law of ALC can be described as

$$u_{j+1}(n) = (1-\alpha)u_j(n) + \Phi(\omega)\cdot e_j(n). \tag{29}$$

In the application of ALC, the learning gains for a set of speed points must be obtained beforehand and the speed points should be distributed evenly in the required speed range. Operating in the decentralized control mode, the proposed ALC scheme needs only one learning gain for each DOF at one speed. The tuning process is simple and no identification process is required. The learning gains for these rotational speeds are then stored in a look-up table. It is clear that the learning gains occupy very little memory space in digital controllers. During operation, the controller can automatically adjust its learning gains according to rotating speeds. For a particular speed, the value of the learning gain can be calculated by linear, high order, or spline interpolations [21] based on the learning gains in the look-up table.

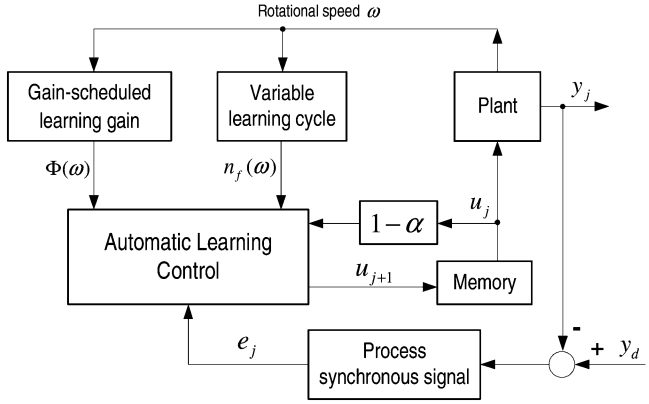

Fig. 5. Automatic learning control scheme.

C. Variable Learning Cycle

In the ILC scheme for AMB unbalance compensation, the length of learning cycle n_f is equal to the constant rotating period, i.e., the time used in one revolution. However, this limits the function of ILC to a specific speed. An iterative learning controller designed for one rotating speed cannot work at another speed. Therefore, this control method is not suitable to the applications where multispeed operation is required. Furthermore, because the controller is only suitable for a fixed speed, it is sensitive to the speed disturbance. In practice, the speed fluctuation always exists due to the external and inner disturbances of the rotating motor and AMB, and error of the speed sensor. The speed disturbance could adversely affect the control performance of ILC. If the speed disturbance is large enough, it could even make the ILC controller fail.

In ALC, the length of learning cycle is not a fixed one. It varies with the variable learning cycle n_f being kept equal to the rotational period of AMB to adapt the controller to the changing speed. The learning law of ALC can thus be described by

$$u_{j+1}(n) = (1-\alpha)u_j(n) + \Phi(\omega)\cdot e_j(n), \quad n \in 0,1,2,\ldots,n_f(\omega)-1 \tag{30}$$

$$n_f(\omega) = 2\pi f_s/\omega \tag{31}$$

where f_s is the sampling frequency.

The proposed ALC scheme is illustrated in Fig. 5.

D. Decentralized Control Mode

The learning law explained in (30) is designed for one-DOF AMB control. As explained in Section II, four radial DOFs are concerned in this paper to realize the unbalance compensation, and therefore there are four inputs and four outputs for the ALC controller. To simplify the control algorithm, the decentralized control mode is used. That is to say, the four-DOF system is divided into four, one-DOF subsystems and the output in one subsystem is only considered in the controller dedicated for that subsystem, as illustrated in Fig. 6. The advantage of decentralized control is obvious as the computational load is reduced up to 75% compared to centralized control mode.

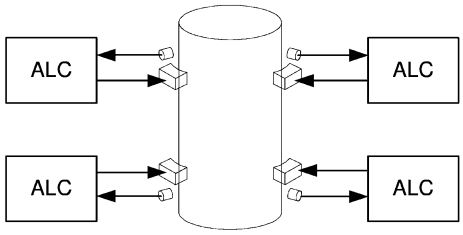

Fig. 6. Decentralized control mode for ALC scheme.

Let $\mathrm{X}_1, \mathrm{X}_2, \mathrm{Y}_1$, and Y_2 represent the radial axes of an AMB system. The ALC law for the decentralized control mode can be expressed as

$$u_{j+1}^{(l)}(n) = (1-\alpha)u_j^{(l)}(n) + \Phi_l(\omega)\cdot e_j^{(l)}(n), \quad l \in (\mathrm{X}_1, \mathrm{X}_2, \mathrm{Y}_1, \mathrm{Y}_2) \quad (32)$$

where l denotes the axis name, $u_j^{(l)}(n)$ is the ALC output for axis l, $e_j^{(l)}(n)$ is the error signal for axis l, and $\Phi_l(\omega)$ is the learning gain for axis l.

E. ALC Scheme for Unbalance Compensation

To reduce the rotor runout, the displacement signal is assigned as the controller input, so the current signal generated by ALC controller should be

$$\begin{aligned} i_{\mathrm{ALC}j+1}^{(l)}(n) &= (1-\alpha)i_{\mathrm{ALC}j}^{(l)}(n) + \Phi_l(\omega)\cdot e_p^{(l)}{}_j(n) \\ &= (1-\alpha)i_{\mathrm{ALC}j}^{(l)}(n) - \Phi_l(\omega)\cdot s_j^{(l)}(n). \end{aligned} \quad (33)$$

To reduce the fluctuations of the coil current, the synchronous current fluctuation is the input of the ALC controller. Therefore, the current signal generated by ALC controller should be

$$\begin{aligned} i_{\mathrm{ALC}j+1}^{(l)}(n) &= (1-\alpha)i_{\mathrm{ALC}j}^{(l)}(n) + \Phi_l(\omega)\cdot e_i^{(l)}{}_j(n) \\ &= (1-\alpha)i_{\mathrm{ALC}j}^{(l)}(n) - \Phi_l(\omega)\cdot i_{\mathrm{syn}j}^{(l)}(n). \end{aligned} \quad (34)$$

The runout and current fluctuation will converge in the learning control process provided that the learning gain satisfies the convergence criteria. Therefore, the compensation scheme can force the rotor to rotate around on the geometric axis or system inertial axis.

The proposed ALC compensation scheme for the AMB unbalance problem is illustrated in Fig. 7. A feedback PID controller, which can be already designed for the optimum transient response, is needed to work together with the ALC controller. The ALC controller is only responsible for providing the unbalance compensation current.

V. Experimental Results

In order to evaluate the proposed automatic learning control scheme, an AMB experiment system, as shown in Fig. 8, is used to test ALC's performance on the rotor runout reduction and current fluctuation reduction, respectively. The diameter of the motor is 50 mm, and its speed can be adjusted to 4000 rpm. Though the system contains a magnetic thrust bearing, it did not affect the radial unbalanced tests designed for verifying the ALC scheme presented. Variable reluctance sensors are used in magnetic bearings to detect the rotor positions. A decentralized PID controller is used in the experiment to stabilize the AMB system. When ALC is turned off, only the PID controller works. When ALC is turned on, it works together with the PID controller.

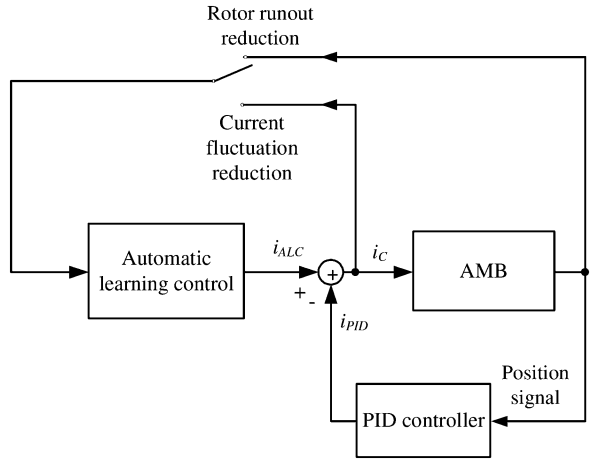

Fig. 7. ALC compensation scheme.

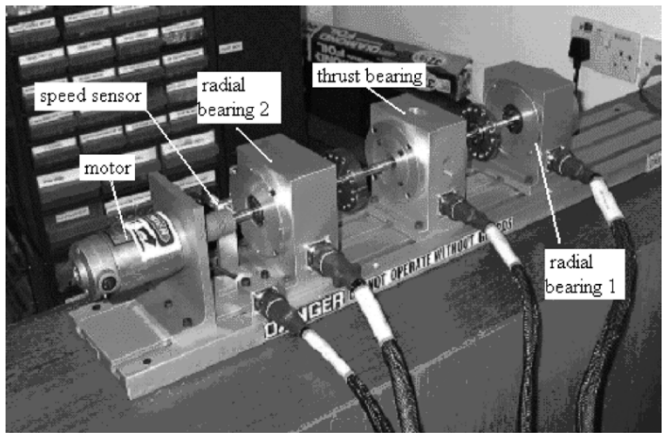

Fig. 8. AMB experimental system.

A dSPACE DS1103 controller board is used to perform real-time digital control on the AMB system. In the experiments, the sampling frequency for A/D conversion is 10 kHz. The bias current i_0 is 1.0 A in the experiment. The force-current factor K_i is 30.45 N/A, and the force-displacement factor K_s is 57.97 N/μm. The mass of the rotor is 1.541 kg.

A. Reducing Rotor Runout

The proposed ALC scheme for realizing the rotation around on the geometric axis is tested in the experiment. The experiment is carried out at a constant speed of 2800 rpm (46.67 Hz). Rotor runouts at the four radial axes with ALC scheme are recorded and compared with those without ALC scheme. A portion of the experimental results are shown in Figs. 9 and 10. The synchronous rotor runout at 46.67 Hz is the target to be minimized. The forgetting factor α is kept equal to 0.005 for enough robustness.

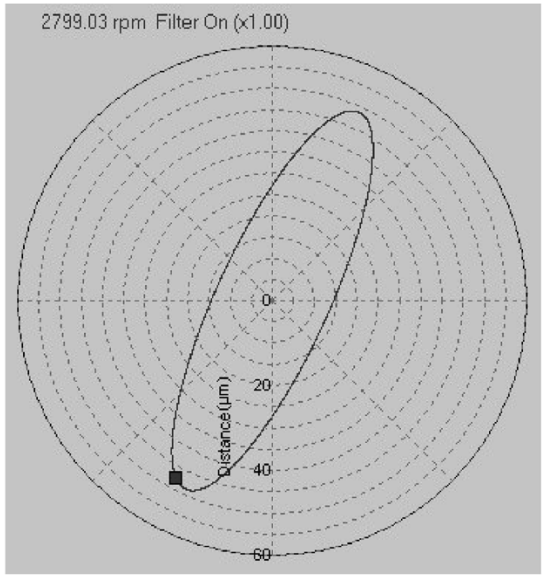

(a)

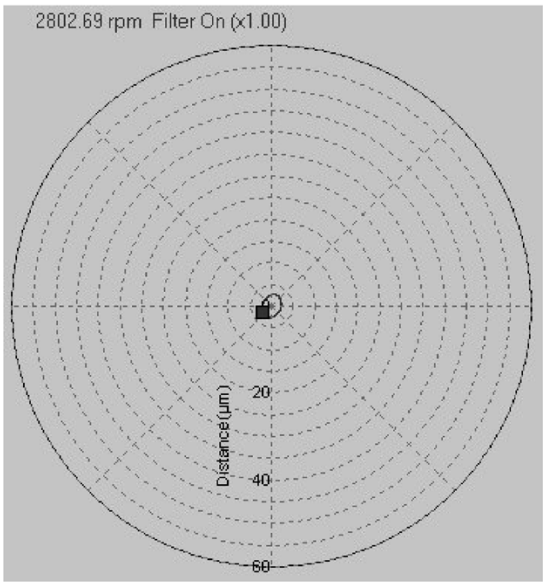

(b)

Fig. 9. Comparison of rotor position orbits. (a) Without ALC scheme. (b) With ALC scheme.

Fig. 9 shows the rotor position orbits (a) without unbalance compensation and (b) with proposed ALC scheme. Without unbalance compensation, the maximum runout is 48 μm. With the effective control of ALC scheme, maximum runout is reduced to 3 μm. The motor speed is controlled at 2800 rpm, and its variation is in range of ± 15 rpm, that is, the speed error is about 0.5%. This speed variation could negatively affect the performance of a conventional ILC controller. However, the ALC compensation scheme presents the satisfactory performance when the speed is fluctuating. This is because ALC could automatically adjust the length of learning cycle according to the rotating speed, so the controller can automatically work at different speeds.

Fig. 10 shows the rotor runout curves in axis X_1 and the corresponding frequency spectrums (a) with only PID control and (b) with ALC scheme. The magnitude of steady-state runout

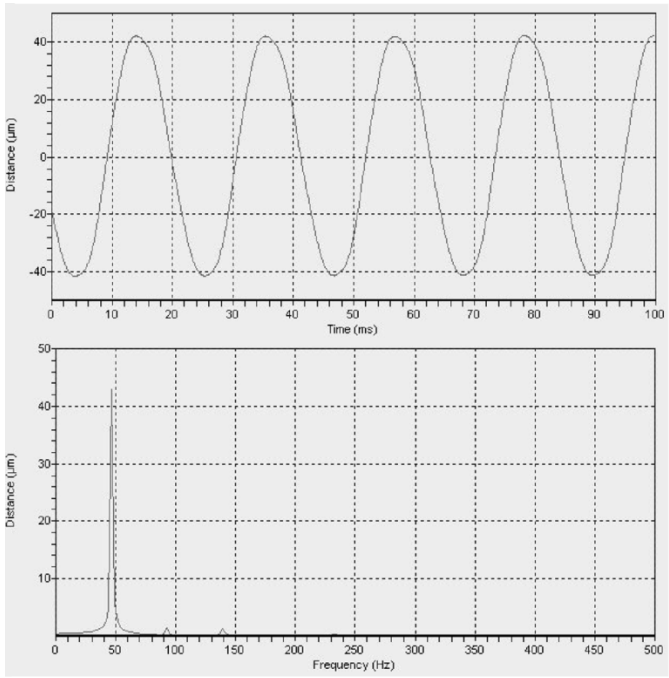

(a)

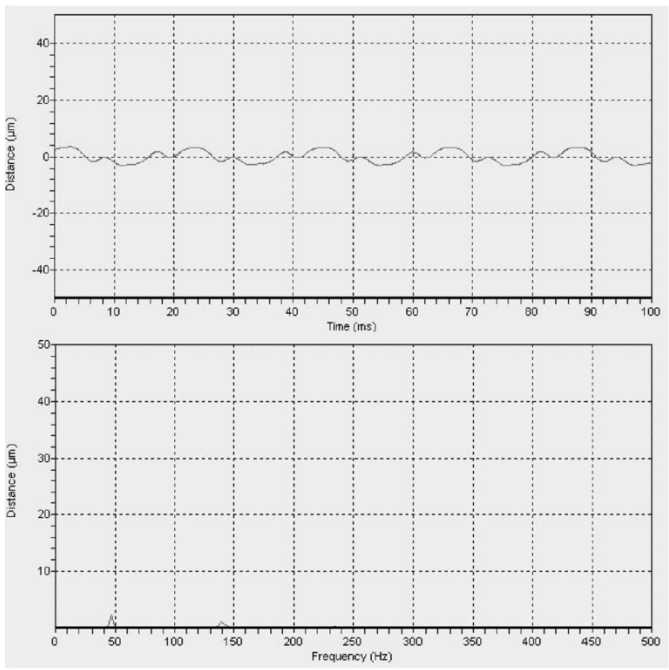

(b)

Fig. 10. Rotor runout in axis X_1 and its frequency spectrum. (a) Without ALC scheme. (b) With ALC scheme.

is 44 μm for PID control, but is only 3.4 μm for ALC control. With the ALC scheme, the synchronous component, the one at 46.67 Hz, is significantly reduced to a very small value. Therefore, the overall runout values decrease substantially in the experiment.

The proposed ALC scheme is also tested in a speed run-up test. The rotating speed rises from 1200 to 3200 rpm. The rotating speed and the peak-to-peak rotor runout values with and without ALC compensation are respectively recorded for comparison. The run-up test result is shown in Fig. 11. The ALC

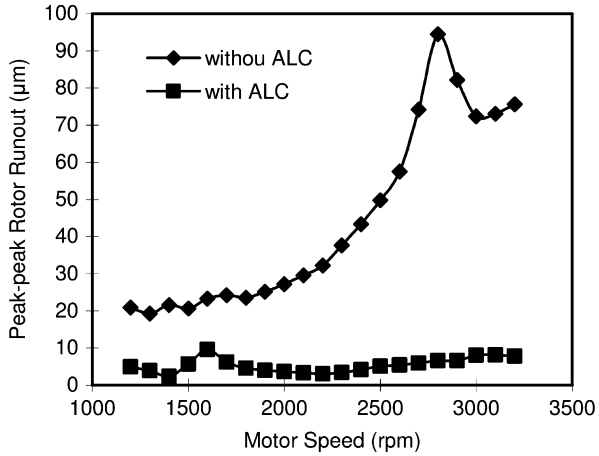

Fig. 11. Rotor position runout values versus rotational speeds.

control scheme exhibits good performance during this experiment. Without ALC, the runout rises dramatically when the rotational speed is approaching 2800 rpm. However, with ALC the runout curve is almost flat and has no obvious difference compared to other speeds.

B. Reducing Coil Current Fluctuation

The proposed ALC scheme is also applied to reduce synchronous coil current fluctuations in AMB coils. Similarly, the experiments are composed of two tests, the constant speed test and the variable speed test. The constant speed test is still carried out at 2800 rpm. The forgetting factor α is 0.005 in both experiments.

The coil currents of one electromagnet in axis X_1 are recorded to compare the performances with and without ALC. The recorded coil currents are the sum of its bias current i_0 and control current i_c. But the coil current in the other electromagnet is the difference of its bias current and control current, as introduced in Section II. However, they have the same fluctuations.

Fig. 12 shows the fluctuations of the recorded coil currents in axis X_1 and the frequency spectrums (a) without ALC and (b) with ALC. The magnitude of current fluctuation without ALC is 0.384 A. With ALC compensation, the magnitude of the current fluctuation is reduced to 0.036 A.

The ALC scheme is also verified to reduce the coil current fluctuations during rotor speed run-up. ALC also presents satisfactory compensation performance in this experiment. Fig. 13 illustrates peak-to-peak values of coil currents fluctuations. It could be seen that the coil current fluctuation decreases substantially when ALC is turned on. In the experiment, the control current without ALC increases a lot when motor speed is approaching the critical speed. With ALC, the fluctuations always maintain within a small value in the experiments.

In addition to attenuate vibrations of machine housing, reducing fluctuations of coil current has another advantage for PM-biased AMB, i.e., reduction of copper loss [14]. Because in PM-biased AMB, bias flux is provided by permanent magnets rather than bias current in classic AMB, there is no bias current in PM-biased AMB. As a result, control current is the only

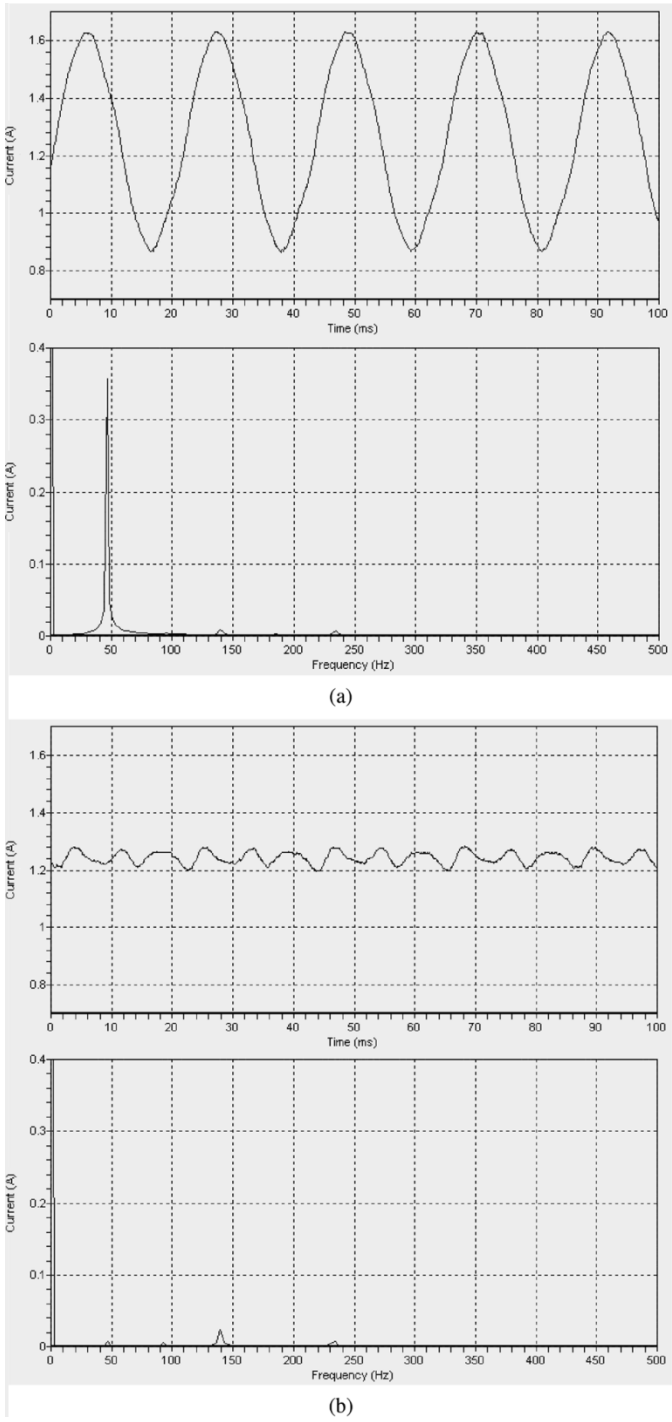

Fig. 12. Fluctuations of coil current and its frequency spectrum. (a) Without ALC. (b) With ALC.

component in electromagnet coils. Copper loss in this kind of AMB is proportional to the square of its effective control current. Thus, its power consumption and generated heat during operation will be reduced significantly by ALC. Smaller control current and less generated heat allow the power electronics to be further integrated, making it possible to put control electronics for small AMB systems in a multichip module (MCM). Fig. 14 shows the comparison of effective values of the control current between ALC off and ALC on. The control current in the latter case can be reduced significantly.

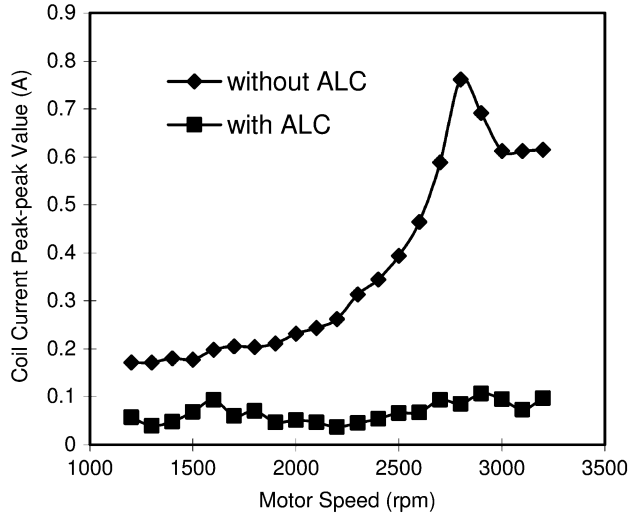

Fig. 13. Fluctuations of coil currents versus rotational speeds.

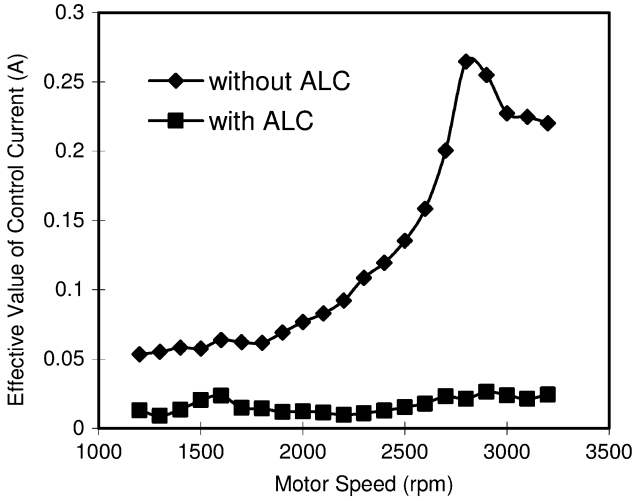

Fig. 14. Effective control currents versus rotational speeds.

C. Discussions

It can be observed that a small amount of rotor runout and control current fluctuations still exist although time-domain ILC or ALC is turned on. The reasons can be explained as follows.

1) The existence of the forgetting factor. According to the analysis before, the forgetting factor in ILC can increase the robustness of the controller with the expense of nonzero steady-state tracking error. Therefore, the forgetting factor should be kept as small as possible provided that the controller robustness is enough for the application requirement.
2) The existence of higher order runout components which are caused by high order repeatable runout and nonrepeatable runout. The unbalance analysis in the previous sections is based on the assumption that the rotor (shaft) is a rigid body. However, this proximity does not consider the characteristics of a flexible body. In a flexible body, higher order harmonics could be excited by the unbalance force and other external forces. The amplitude of the excited vibrations depends on flexible body characteristics, the excitation frequency of the disturbance, and characteristics of applied controllers. In the frequency plots of the experimental results, higher order runout components and AMB coil currents can be observed, but only the synchronous component is managed to be eliminated. The higher order components of rotor runouts and control current fluctuations are left unprocessed. These residual higher order components can be further processed to meet higher operation requirements. For example, if the higher order components could be obtained from the filter and input to the ALC controller, the controller could suppress the higher order components as well as synchronous components in the iterative learning process.
3) Transient response during rotational speed fluctuations or unbalance conditions changes. Changes of unbalance conditions or rotational speed could result in the variation of control effects. During the process of speed changing, the transient rotor runout or coil current fluctuation could increase temporarily in the ALC scheme and come back to steady state very quickly. Because ALC is designed insensitive to the rotating speed fluctuation, the influence of speed variation is minimized.

VI. Conclusion

In this paper, the unbalance problems in AMB are analyzed. The unbalance forces exist in the AMB system and they can induce the rotor runout and the fluctuations of the AMB control current, which are undesirable in applications. An effective control method, automatic learning control, is proposed to compensate the unbalance effects to reduce rotor runout and coil current fluctuations. The ALC scheme is developed from time-domain ILC and has the ability to work in a predetermined wide-speed range. During operation, ALC can automatically adjust its learning gain and cycle to make itself suitable for different speeds. Experimental results prove that ALC can significantly reduce the rotor runout as well as the fluctuations of AMB control current. ALC is more robust than the ILC to the disturbance of the rotor speed.

Appendix

In order to introduce the discrete model as shown in (20), the DOF of axis X is taken as an example to obtain the elements of matrices $\mathbf{A}, \mathbf{B}$, and $\mathbf{C}$. To be simple, the index of the axis x is omitted. First, the control current of AMB in the continuous combined ALC and PID plant can be expressed as

$$i_c(t) = -k_P s(t) - k_D \dot{s}(t) - k_I \int_0^t s(\tau)\, d\tau + i_{\mathrm{ALC}}(t). \quad (35)$$

The motion equation is

$$\begin{aligned} \ddot{s} = &-\frac{K_i k_D}{m}\dot{s} + \left(\omega^2 + \frac{K_s}{m} - \frac{K_i k_p}{m}\right) s \\ &- \frac{K_i k_I}{m}\left(\int_0^t s(\tau)\, dt + \frac{i_{c0}}{k_I}\right) \\ &+ \frac{K_i}{m}\cdot i_{\mathrm{ALC}} + \varepsilon\cos(\omega t + \theta)\omega^2. \end{aligned} \quad (36)$$

Let $\mathrm{x}_1 = \mathrm{s}, \mathrm{x}_2 = \dot{s}, \mathrm{x}_3 = \int_0^t s(\tau)\,d\tau + ((i_{c0})/(k_I)), \mathbf{X} = [x_1\ x_2\ x_3]^T$, then

$$\frac{d}{dt}\mathbf{X} = \begin{bmatrix} 0 & 1 & 0 \\ \omega^2 + \frac{K_s}{m} - \frac{K_i k_p}{m} & -\frac{K_i k_D}{m} & -\frac{K_i k_I}{m} \\ 1 & 0 & 0 \end{bmatrix} \mathbf{X} + \begin{bmatrix} 0 & 0 \\ \frac{K_i}{m} & 1 \\ 0 & 0 \end{bmatrix} \begin{bmatrix} i_{\mathrm{ALC}} \\ \varepsilon \cos(\omega t + \theta)\omega^2 \end{bmatrix}. \quad (37)$$

Assume

$$\mathbf{A}_c = \begin{bmatrix} 0 & 1 & 0 \\ \omega^2 + \frac{K_s}{m} - \frac{K_i k_p}{m} & -\frac{K_i k_D}{m} & -\frac{K_i k_I}{m} \\ 1 & 0 & 0 \end{bmatrix}, \mathbf{B}_c = \begin{bmatrix} 0 & 0 \\ \frac{K_i}{m} & 1 \\ 0 & 0 \end{bmatrix},$$
$$\mathbf{u} = \begin{bmatrix} i_{\mathrm{ALC}} \\ \varepsilon \cos(\omega t + \theta)\omega^2 \end{bmatrix}, \mathbf{Y} = [s] \text{ and } \mathbf{C}_c = [1 \quad 0 \quad 0] \quad (38)$$

then the continuous-time ALC closed-loop AMB system can be described by

$$\begin{cases} \dfrac{d}{dt}\mathbf{X}(t) = \mathbf{A}_c \cdot \mathbf{X}_c(t) + \mathbf{B}_c \cdot \mathbf{u}(t) \\ \mathbf{Y}(t) = \mathbf{C}_c \cdot \mathbf{X}(t) \end{cases}. \quad (39)$$

The discrete-time closed-loop AMB system is

$$\begin{cases} \mathbf{X}(n) = \mathbf{A} \cdot \mathbf{X}(n-1) + \mathbf{B} \cdot \mathbf{u}(n-1) \\ \mathbf{Y}(n) = \mathbf{C} \cdot \mathbf{X}(n) \end{cases} \quad (40)$$

where $\mathbf{A} = e^{\mathbf{A_c} T_s} = \sum_{j=0}^{\infty} (\mathbf{A_c}^j T_s^j)/(j!)), T_s$, the sampling interval

$$\mathbf{B} = \int_0^{T_s} e^{\mathbf{A_c}(T_s - \tau)}\,d\tau \cdot \mathbf{B}_c = \left(\sum_{j=0}^{\infty} \frac{\mathbf{A_c}^j T_s^{j+1}}{(j+1)!} \right) \cdot \mathbf{B}_c,$$
$$\text{and} \quad \mathbf{C} = \mathbf{C}_c. \quad (41)$$

For the DOF of axis Y, the input of the module is

$$\mathbf{u}_y = \begin{bmatrix} i_{\mathrm{ALC}y} \\ \varepsilon \sin(\omega t + \theta)\omega^2 \end{bmatrix}. \quad (42)$$

In this way, the discrete modules of all DOFs can thus be built up.

REFERENCES

[1] P. L. Tímár, Ed., *Noise and Vibration of Electrical Machines*. Amsterdam, The Netherlands: Elsevier, 1989.

[2] C. R. Knospe, R. W. Hope, S. J. Fedigan, and R. D. Williams, "Experiments in the control of unbalance response using magnetic bearings," *Mechatronics*, vol. 5, pp. 385–400, 1995.

[3] R. Herzog, P. Buhler, C. Gahler, and R. Larsonneur, "Unbalance compensation using generalized notch filters in the multivariable feedback of magnetic bearings," *IEEE Trans. Contr. Syst. Technol.*, vol. 4, no. 5, pp. 580–586, Sep. 1996.

[4] F. Matsumura, M. Fujita, and K. Okawa, "Modeling and control of magnetic bearing systems achieving a rotation around the axis of inertia," in *Proc. 2nd Int. Symp. Magnetic Bearings*, Tokyo, Japan, Jul. 12–14, 1990, pp. 273–280.

[5] T. Mizuno and T. Higuchi, "Design of magnetic bearing controllers based on disturbance estimation," in *Proc. 2nd Int. Symp. Magnetic Bearings*, Tokyo, Japan, Jul. 12–14, 1990, pp. 281–288.

[6] B. Shafai, S. Beale, P. LaRocca, and E. Cusson, "Magnetic bearing control systems and adaptive forced balancing," *IEEE Control Syst. Mag.*, vol. 14, no. 2, pp. 4–13, Apr. 1994.

[7] J. Shi, R. Zmood, and L. Qin, "Synchronous disturbance attenuation in magnetic bearing systems using adaptive compensation signals," *Control Eng. Practice*, vol. 12, no. 3, pp. 283–290, Mar. 2004.

[8] J. D. Setiewan, R. Mukherjee, and E. H. Maslen, "Synchronous sensor runout and unbalance compensation in active magnetic bearings using bias current excitation," *Trans. ASME, J. Dyn. Syst., Meas. Control*, vol. 124, no. 1, pp. 14–24, 2002.

[9] T. Higuchi, M. Otsuka, T. Mizuno, and T. Ide, "Application of periodic control with inverse transfer function compensation in totally active magnetic bearings," in *Proc. 2nd Int. Symp. Magnetic Bearing*, Tokyo, Japan, Jul. 12–14, 1990.

[10] C. R. Knopse, S. M. Tamer, and S. J. Fedigan, "Synthesis of robust gain matrices for adaptive rotor vibration control," *Trans. ASME, J. Dyn. Syst., Meas. Control*, pp. 298–300, Jun. 1997.

[11] C. Bi, D. Z. Wu, Q. Jiang, and Z. J. Liu, "Optimize control current in magnetic bearings using automatic learning control," in *Proc. IEEE Int. Conf. Mechatronics*, Istanbul, Turkey, Jun. 3–5, 2004.

[12] G. Schweitzer, H. Bleuler, and A. Traxler, *Active Magnetic Bearings: Basics, Properties, and Applications of Active Magnetic Bearings*. Zurich, Switzerland: vdf Hochschulverlag, 1994.

[13] C. K. Sortore, P. E. Allaire, E. H. Maslen, R. R. Humphris, and P. A. Studer, "Permanent magnet biased magnetic bearings-design, construction, and testing," in *Proc. 2nd Int. Symp. Magnetic Bearings*, Tokyo, Japan, Jul. 1990, pp. 175–182.

[14] F. Betschon, "Design principle of integrated magnetic bearings," Ph.D. dissertation, Nr. 13643, ETH, Zürich, Switzerland, 2000.

[15] S. Arimoto, S. Kawamura, and F. Miyazaki, "Bettering operation of robots by learning," *J. Robot. Syst.*, vol. 1, no. 2, pp. 123–140, 1984.

[16] Z. Bien and J. Xu, *Iterative Learning Control: Analysis, Design, Integration, and Applications*. Norwell, MA: Kluwer, 1998.

[17] W. Qian, S. K. Panda, and J. X. Xu, "Torque ripple minimization in PM synchronous motors using iterative learning control," *IEEE Trans. Power Electron.*, vol. 19, no. 2, pp. 272–279, Mar. 2004.

[18] R. W. Longman, M. Q. Phan, J.-N. Juang, and R. Ugoletti, "Simple learning control made practical by zero-phase filtering: Applications to robotics," *IEEE Trans. Circuits Syst. I: Fundam. Theory Appl.*, vol. 49, no. 6, pp. 753–767, Jun. 2002.

[19] R. W. Longman, "Designing iterative learning and repetitive controllers," in *Iterative Learning Control: Analysis, Design, Integration, and Applications*, Z. Bien and J. X. Xu, Eds. Norwell, MA: Kluwer, 1998, ch. 7, pp. 107–146.

[20] S. Arimoto, T. Naniwa, and H. Suzuki, "Robustness of P-type learning control with a forgetting factor for robotic motions," in *Proc. 29th IEEE Conf. Decision and Control*, vol. 5, Dec. 1990, pp. 2640–2645.

[21] A. Wood, *Introduction to Numerical Method*. Reading, MA: Addison-Wesley, 1999.

Manuscript received March 7, 2005; revised May 5, 2005.

Chao Bi (M'92) received the B.Eng. degree from the Hefei University of Technology, Hefei, China, in 1982, the M.Eng. degree from Xian Jiaotong University, Xian, China, in 1984, and the Ph.D. degree from the National University of Singapore, Singapore, in 1994.

He is presently a Research Scientist at the Data Storage Institute, Singapore, and concurrent lecturer of the National University of Singapore. His research interests include the design, control, and test of permanent-magnet motor, design and control and test of microactuator, micromotor technology, electromagnetic field synthesis and analysis, and optimization technology. He has published more than 50 conference and journal papers in these areas.

Dezheng Wu (S'05) received the B.Eng. degree in electrical engineering from Shanghai Jiao Tong University, Shanghai, China, in 2000 and the M.S. degree from the National University of Singapore, Singapore, in 2005. He is currently working toward the doctoral degree at Michigan State University, East Lansing.

From 2000 to 2002, he was with Dahua Energy Technological Company as an Electrical Engineer. From 2002 to 2004, he was with the Data Storage Institute, Singapore, and the National University of Singapore. His research interests include control systems, design and control of electromechanical systems and motor drives.

Quan Jiang (M'03) received the B.Eng. degree from Hefei University of Technology, Hefei, China, in 1983 and the M.Eng. and Ph.D. degrees from Southeast University, Nanjing, China, in 1986 and 1991, respectively.

He worked as a Postdoctoral Fellow/Research Associate at the University of Hong Kong, Hong Kong, from 1994 to 2000. He is now a Senior Engineer at the Data Storage Institute, Singapore. His research interests are in design, control and testing of electric machines, electric drives, power electronics, finite-element analysis of electromagnetic field, and applications of micro-controller, DSP, and FPGA devices. He has worked extensively on research of HDD spindle motors and drives, switched reluctance motor and drives, synchronous motors, and dc motors. He has published more than 50 academic papers and coauthored two chapters of two books.

Zhejie Liu (SM'93) was born in Jiangsu, China. He received the B.Eng. degree in electrical engineering from Hefei University of Technology, Hefei, China, in 1982 and the Ph.D. degree from Liverpool University, Liverpool, U.K., in 1992.

In 1992 and 1993 he worked as a Postdoctoral Research Associate at Sheffield University, Sheffield, U.K., in the area of computer-aided design of permanent magnet motors and drives. He is presently a Research Scientist at the Data Storage Institute, Singapore. His research interests include magnetic materials, electric machines and actuators, design optimization, CAD/CAE, magnetic recording, micromagnetic modeling and simulation, and HF electromagnetic fields.